FEMS Yeast Research, 18, 2018, foy052

doi: 10.1093/femsyr/foy052
Advance Access Publication Date: 26 April 2018
Research Article

RESEARCH ARTICLE

Cell size and morphological properties of yeast *Saccharomyces cerevisiae* in relation to growth temperature

Maksim Zakhartsev[1,2,3,*,†] and Matthias Reuss[2]

[1]Centre for Integrative Genetics, Norwegian University of Life Sciences, Arboretveie 6, 1432 Ås, Norway, [2]Stuttgart Research Center Systems Biology (SRCSB), University of Stuttgart, Nobelstrasse 15, 70569 Stuttgart, Germany and [3]Department of Biotechnology, Ural Federal State University, Mira 28, 620002 Ekaterinburg, Russia

*Corresponding author: Dr. Maksim Zakhartsev, Centre for Integrative Genetics, Norwegian University of Life Sciences, Arboretveien 6, 1432 Ås, Norway. Tel: + 47 67 232 607; E-mail: maksim.zakhartsev@nmbu.no
One sentence summary: The yeast cell size, intracellular morphology and population structure vary in course of the glucose unlimited anaerobic batch growth in regard to the growth temperature.
Editor: Jens Nielsen
†Maksim Zakhartsev, http://orcid.org/0000-0002-7973-9902

ABSTRACT

Cell volume is an important parameter for modelling cellular processes. Temperature-induced variability of cellular size, volume, intracellular granularity, a fraction of budding cells of yeast Saccharomyces cerevisiae CEN.PK 113–7D (in anaerobic glucose unlimited batch cultures) were measured by flow cytometry and matched with the performance of the biomass growth (maximal specific growth rate (μ_{max}), specific rate of glucose consumption, the rate of maintenance, biomass yield on glucose). The critical diameter of single cells was 7.94 μm and it is invariant at growth temperatures above 18.5°C. Below 18.5°C, it exponentially increases up to 10.2 μm. The size of the bud linearly depends on μ_{max}, and it is between 50% at 5°C and 90% at 31°C of the averaged single cell. The intracellular granularity (side scatter channel (SSC)-index) negatively depends on μ_{max}. There are two temperature regions (5–31°C vs. 33–40°C) where the relationship between SSC-index and various cellular parameters differ significantly. In supraoptimal temperature range (33–40°C), cells are less granulated perhaps due to a higher rate of the maintenance. There is temperature dependent passage through the checkpoints in the cell cycle which influences the μ_{max}. The results point to the existence of two different morphological states of yeasts in these different temperature regions.

Keywords: budding yeast; cellular size; cellular volume; growth temperature; anaerobic batch growth; surface-to-volume ratio; intracellular morphology; intracellular granularity; cell cycle; maintenance

INTRODUCTION

Cell volume is an important parameter for mathematical modeling of the metabolic cellular processes (Reich and Selkov 1981; Theobald 1995; Stephanopoulos, Aristidou and Nielsen 1998; Villadsen, Nielsen and Liden 2011). Cells are three-dimensional particles (Fig. 1A) and therefore characterized by a surface area through which the exchange/transport processes (*i.e.* metabolic fluxes) are occurring between extra- and intra-cellular volumes. From physical-chemical point of view, a material flux (J) across

Received: 27 February 2018; **Accepted:** 25 April 2018

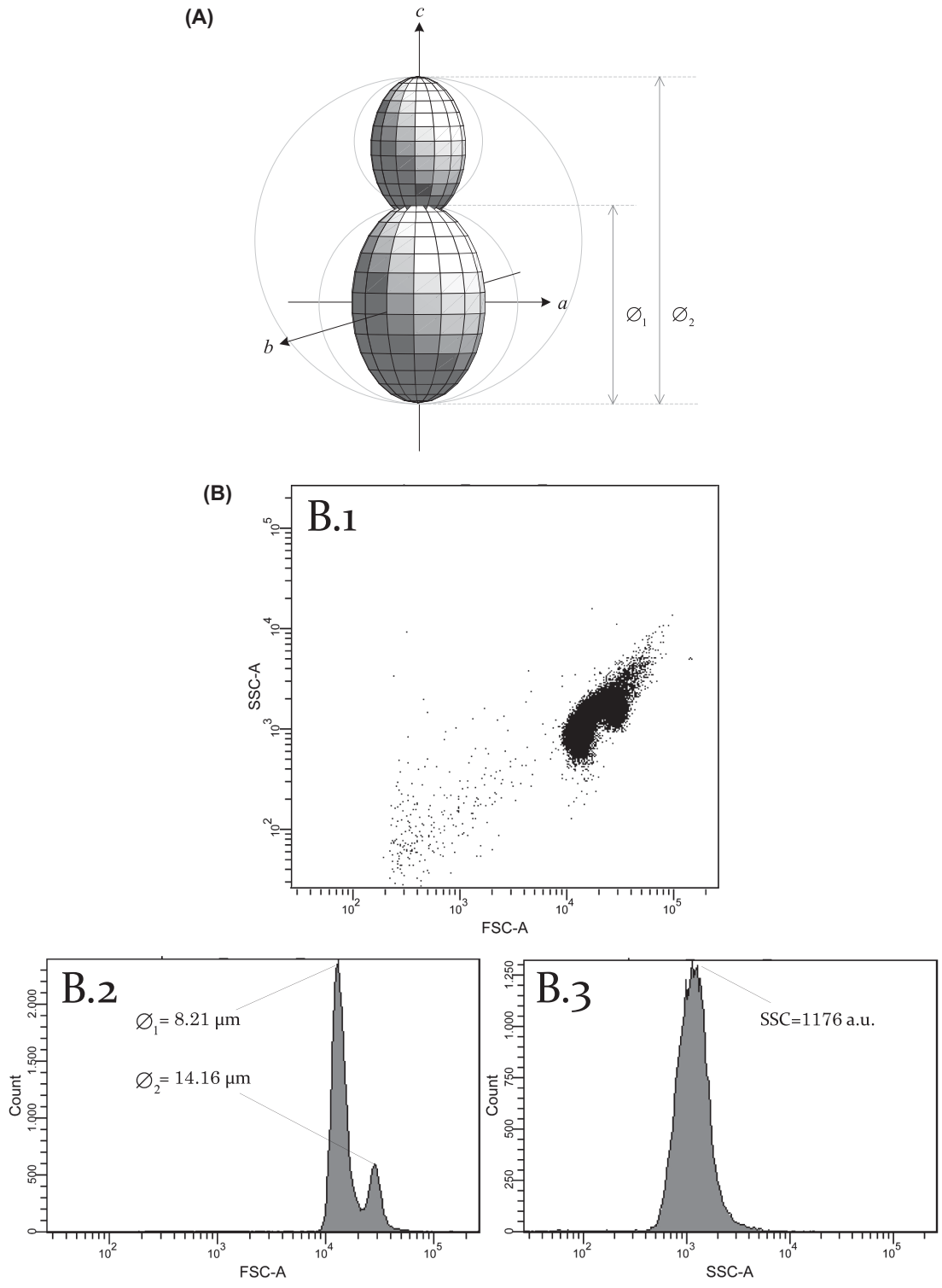

Figure 1. (A) The cells of yeast *Saccharomyces cerevisiae* are prolate spheroids ($a = b < c$). Therefore, roughly, the budding yeast cells can be geometrically approximated as two spheres (mother + bud), whose sizes can be measured by flow cytometry. $\emptyset_i$ —average cell diameter [μm]. There are two cell fractions in intact (i.e. non-stained and un-sonicated) yeast cell suspension: (i) cells with $\emptyset_1$ —single mother (*m*) cells in G_1 growth phase; (ii) cells with $\emptyset_2$– budding (*m* + *bud*) cells in S/G_2/*M* growth phases. (B) An example of the flow cytometry of intact (*i.e.* non-stained and un-sonicated) yeast *Saccharomyces cerevisiae* CEN.PK 113–7D culture grown in glucose unlimited anaerobic batch at 26.3°C (for details of the growth conditions see Fig. 2): (B.1) distribution of cell population in FSC/SSC space, cell count = 5×10^4; (B.2) distribution of the forward scatter signal (FSC), the cell diameter ($\emptyset$, in μm) was calculated after calibration of the FSC channel with the standard beads (1–15 μm). Details of the analysis of the fractions are presented in Fig. S1 (Supporting Information). In this example, 30% of the cell population are budding cells (in S/G_2/*M* phases) and the rest are growing single mother cells (in G_1 phase); (B.3) distribution of the side scatter signal (SSC), which is the measure of the cell granularity expressed in arbitrary units [*a.u.*].

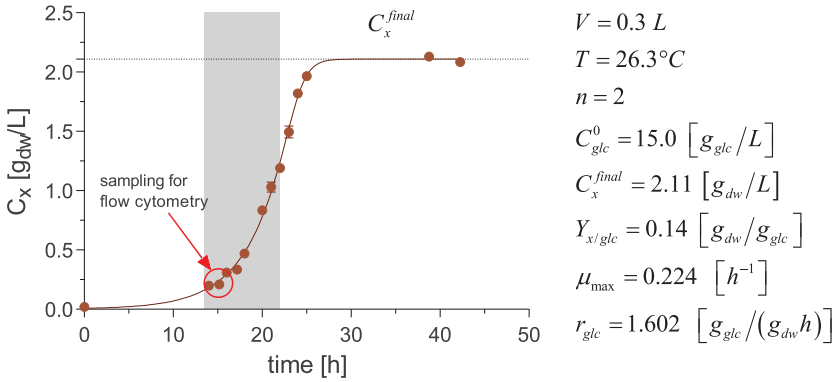

Figure 2. An example of the anaerobic glucose-unlimited batch growth of yeast *Saccharomyces cerevisiae* CEN.PK 113–7D in shaking flask at 26.3°C. Such growth experiments were performed at different isothermal conditions within 5–40°C temperature range. The shaded area indicates time period within which the culture has reached maximum specific growth rate (μ_{max}), and where samples for flow cytometry were taken. Where: C_x— biomass concentration [g_{dw}/L_R]; C^0_{glc}— initial glucose concentration [g_{glc}/L_R]; C_x^{final} – final biomass concentration achieved at the end of the batch growth, when glucose is completely exhausted [g_{dw}/L_R]; — biomass yield on glucose [g_{dw}/g_{glc}]; μ_{max} — maximal specific growth rate [1/*h*]; r_{glc} — specific glucose consumption rate [$g_{glc}/(g_{dw}h)$]; *dw*—dry weight; *glc*—glucose.

cellular membrane is a rate of flow of a property per unit area [$mol/(m^2 \times h)$]. However, due to lack of information on volumetric properties of biological objects, the in-/output fluxes from microbial biomass are usually expressed in units of biomass specific rates (*r*) [$mol/(g_{dw} \times h)$], which are practically measured in experiments. The *J* and *r* are bound through an intracellular density of biomass (ρ_x) and surface-to-volume ratio of a cell (S_{TS}/V_{TV}):

$$J = \frac{r \cdot \rho_x}{(S_{TS}/V_{TV})} \quad (1)$$

where: *J* —a flux of a metabolite [$mol/(m^2 \times h)$]; *r*—biomass specific rate of a metabolite transport [$mol/(g_{dw} \times h)$]; ρ_x —density of biomass [g_{dw}/L_{TV}]; S_{TS}—total approximated surface area of an averaged cell in population [m^2]; V_{TV}—total approximated cell volume of an averaged cell [L_{TV}] (equation (6)); S_{TS}/V_{TV}—surface-to-volume ratio of a cell [m^2/L_{TV}]. It is important to note, that the ρ_x is expressed in units of weight of the dry biomass per volume of the fresh biomass.

The volumetric properties (such as ρ_x and S_{TS}/V_{TV}) of the studying cells are often unknown and therefore they must be either empirically obtained or estimated from the common knowledge. For example, ρ_x of yeast *Saccharomyces cerevisiae* was estimated to be approximately 300 [g_{dw}/L_{TV}] (Theobald 1995) (the details of that estimation are provided in Supplement 1, Supporting Inforamtion).

It is obvious that the population of cells, where cells are three-dimensional particles (Fig. 1A) which are filled with an intracellular content, making up the total biomass in a reaction volume (V_R). Thus, the total mass of all cells in the cultural volume (*i.e.* biomass concentration) is the product of cell concentration (*N*), total approximated cell volume of an averaged cell (V_{TV}) and averaged density of a biomass (ρ_x):

$$C_x = N \cdot V_{TV} \cdot \rho_x \quad (2)$$

Where: C_x—concentration of the dry biomass [g_{dw}/L_R]; *N*—cell concentration [n/L_R]. Thus, ρ_x can be accurately derived from the experimental measurements of the biomass concentration, cell concentration and known volumetric properties of cells.

Taking into account equation (2), the increment of the biomass in course of the exponential growth phase of the microbial culture (exemplified in Fig. 2) integrates all these parameters:

$$\frac{dC_x}{dt} = \mu_{max} \cdot C_x = \mu_{max} \cdot N \cdot V_{TV} \cdot \rho_x \quad (3)$$

Where: μ_{max}—maximum specific growth rate of dry biomass [$g_{dw}/(g_{dw} \times h)$] or [h^{-1}].

Optical methods are often employed for estimation of the biomass properties. The most common optical method is a measurement of the light scattering exerted by a population of cells, *i.e.* so-called optical density (OD) of cellular culture (Hulst 1957). Under invariant growth conditions (when the cell size/shape and their internal content are assumed to be almost invariant) the OD method can be employed to estimate the cell or biomass concentration after calibration under specific growth conditions (Burke, Dawson and Stearns 2000). However, the OD method integrates all terms of the equation (2) simultaneously. From the other side, the modern high-throughput optical techniques (*e.g.* flow cytometry; FC) allow measuring optical properties of individual cells and then integrating the properties at the population level. This allows estimating the separate contribution of each factor from equation (2) and estimate their variability.

However, the natural variability of the parameters in equation (2) is unknown. From the other side, it is well documented that some parameters of the yeast biomass vary under different growth temperatures, for example, the biomass specific growth rate μ_{max}, the rate of the intracellular maintenance and, as the consequence, the biomass yield on substrate ($Y_{x/s}$) (Roels 1983; Stephanopoulos, Aristidou and Nielsen 1998; Villadsen, Nielsen and Liden 2011; Zakhartsev *et al.* 2015). Therefore the question arises whether the parameters in equation (2) can vary with variation of growth temperature and have contribution to the overall temperature dependence of the biomass growth rate (equation (3)).

Variation of μ_{max} and N

The temperature dependence of microbial μ_{max} observed within permissive growth temperatures (it is between 3°C and 42°C for genus *Saccharomyces* (Piper 1996; Salvado *et al.* 2011)) is often approximated through the Arrhenius equation, which

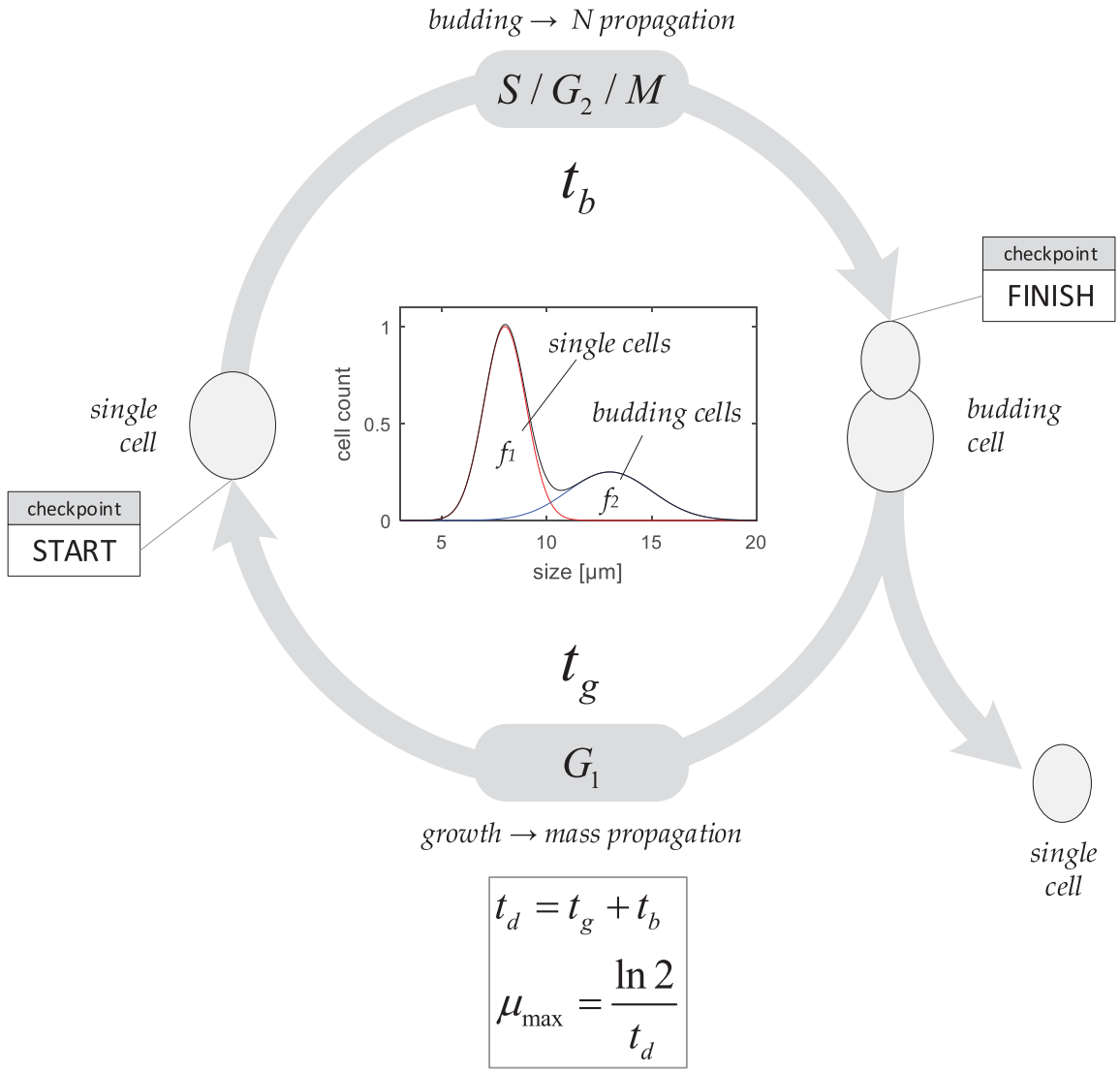

Figure 3. Simplified view on yeast cell cycle assuming substrate unlimited exponential batch growth. At the population level, the cell number (N, equation (3)) propagates due to budding in course of the S/G_2/M-phases, whereas weight of the biomass ($V_{TV} \cdot \rho_x$, equation (3)) propagates due to cell growth in course of the G_1-phase. The temperature effect on the durations of both phases of cell cycle and consequently on μ_{max} (equation (4)) can be carried out through both (i) direct temperature effect on the kinetics of the biochemical reactions and (ii) temperature induced perturbations of the passage through the START and FINISH checkpoints in the cell cycle, which is reflected in the fractional ratio of single (f_1) and budding (f_2) cells in the population under giving conditions. Where: G_1 – G_1-growth phase; S/G_2/M—S/G_2/M-growth phases, *i.e.* budding phase; START—G_1-checkpoint; FINISH—spindle assembly checkpoint; t_d—doubling time of the biomass [*h*], assuming exponential growth (equation (4)); t_d—duration of the S/G_2/M-phase, *i.e.* budding period [*h*] (equation (7)); t_g—duration of the G_1-phase, *i.e.* period of growth to reach critical volume and to prepare for a new division cycle [*h*]; *mass*—mass of cells.

describes temperature effect on the kinetics of the key molecular processes in the cell growth (Roels 1983; Stephanopoulos, Aristidou and Nielsen 1998; Nielsen, Villadsen and Liden 2003; Villadsen, Nielsen and Liden 2011). From the other side, the μ_{max} can be decomposed onto sum of durations of cell cycle phases, particularly cell division (*i.e.* budding) and post-mitotic growth (equation (4); Fig. 3) (Porro *et al.* 2009) with their corresponding individual temperature dependencies (Vanoni, Vai and Frascotti 1984):

$$\mu_{max}(T) = \frac{\ln 2}{t_d(T)} = \frac{\ln 2}{t_b(T) + t_g(T)} \quad (4)$$

Where: t_d—doubling time of the biomass [*h*]; t_b—duration of the S/G_2/M-phase, *i.e.* budding period [*h*] (equation (7)); t_g—duration of the G_1-phase, *i.e.* period of growth to prepare for a new division cycle [*h*]. The phases of the cell cycle are separated by molecular control mechanisms (*e.g.* checkpoints) that ensure proper division of the cell (Porro *et al.* 2009). There are two major checkpoints in yeast cell cycle (Fig. 3): (i) G_1 or so-called Start and (ii) spindle assembly or so-called Finish (Chen *et al.* 2004). There are several known criteria for passing each checkpoint. Moreover, it is known that the temperature dependence of each phase of cell cycle can be different. For example, it was shown that duration of S-phase of yeast *Saccharomyces cerevisiae* is almost temperature insensitive between 20°C and 40°C, while it linearly increases below 20°C towards 5°C (Vanoni, Vai and Frascotti 1984). The dividing cell can be arrested in either of the checkpoints of the cell cycle until the fulfilment of the required passage criteria. Thus, temperature dependencies

of the control mechanisms in different checkpoints can differently contribute to the overall temperature dependency of the μ_{max} (Vanoni, Vai and Frascotti 1984; Porro *et al.* 2009). Consequently, the arrest of cell cycle in any checkpoints due to temperature effect must be reflected in variation of *N* and fractional ratio of budding/single cells.

Thus, the temperature dependence of duration of the cell cycle (*i.e.* biomass specific growth rate μ_{max}) is the superposition of two major processes:

i. temperature effect on rates of all biochemical reactions involved in both G_1- and $S/G_2/M$ phases of the cell cycle (expressed through the Arrhenius equation), *i.e.* cell growth.
ii. temperature dependent passage through the checkpoints in the cell cycle, *i.e.* cell division.

The last process contributes to the regulation of ratio between G_1- and $S/G_2/M$ phases, which together defines the fraction of budding cells in the culture (Hartwell 1974) (Fig. 3, equation (4)).

Variation of V_{TV}

There is a natural variability of a cellular sizes, which ideally should result in the normal Gaussian distribution of this parameter within the cell population (Figs 1B and 3). There is a critical cell size/volume [$V_{TV}^{critical}$] that microbial cells must reach in order to initiate the cell division. Apparently, the mean of the size distribution of the single cells in population corresponds to the critical size of a given microorganism.

In the yeast cell cycle, gaining the critical cell size is one of the passage criteria among others to pass through the G_1-checkpoint to start budding. We can expect that under temperature variation, that $V_{TV}^{critical}$ can vary due to complexity of the passing criteria. For example, if a cell has reached the critical size, but still is arrested in the G_1-checkpoint due to actuality of other passage criteria, then obviously a cell can keep on growing until the limiting passage criteria is fulfilled. Therefore, the G_1-growth phase elongates and correspondingly a cell can reach larger cellular volume (*i.e.* V_{TV}). However, according to our knowledge, there is no systematic research on the investigation of cell size variability of yeast *Saccharomyces cerevisiae* under different temperature growth conditions.

Variation of ρ_x

It is well documented that macromolecular composition of growing microbial cells varies in relation to the growth rate (Roels 1983; Stephanopoulos, Aristidou and Nielsen 1998; Villadsen, Nielsen and Liden 2011), which means that the variation of the density of packaging of the intracellular content (ρ_x) is expected. For example, in glucose-limited continuous cultures of yeast *Saccharomyces cerevisiae*, at low μ_{max} ($<0.1\ h^{-1}$) the carbohydrates content is up to ~50% of the dry biomass and proteins content is up to ~40% of the dry biomass, whereas at high μ_{max} ($>0.3\ h^{-1}$) the carbohydrates content linearly decreases down to ~15% and proteins content increases up to ~60% of the dry biomass (Nissen *et al.* 1997; Lange and Heijnen 2001). The carbohydrates mainly stored in form of glycogen granules in the yeasts, which makes the cytosol optically inhomogeneous. At the same time, it is known that content of intracellular organelles also varies in dependence on the environmental factors. For example, high content of ribosomes was observed in some microbes at low growth rates (Farewell and Neidhardt 1998). Thus, these facts give a reason to expect that the intracellular granularity detected by optic methods should become higher at slow growth rates. Therefore, it is expected that temperature induced variation in μ_{max} must be reflected in variability of the intracellular content (*i.e.* macromolecular composition, content of organelles, content of various deposits, *etc*) of yeast cells, which obviously can be detected by FC as the varying intracellular morphological complexity or so-called intracellular granularity. Therefore, it is expected that ρ_x can vary in dependence on μ_{max}. To our knowledge, there is no systematic information on the variability of intracellular morphology in dependence on the growth temperature.

According to our knowledge, the variability of V_{TV}, S_{TS} and ρ_x are not systematically investigated. Therefore, the goal of this research is to estimate the variability of yeast *Saccharomyces cerevisiae* cellular volumetric and morphological properties in anaerobic batch cultures under different growth temperatures.

MATERIALS AND METHODS

Yeast strain and medium

Baker yeast *Saccharomyces cerevisiae* haploid strain CEN.PK 113–7D (*MATa*, *Ura3*, *His3*, *Leu2*, *Trp1*, *Mal2*, *Suc2*; kindly provided by Dr. Peter Kötter, Institute for Molecular Biosciences, Göthe University of Frankfurt, Germany) was used in the experiments. Minimal mineral medium (so-called CEN.PK medium) was used for yeast cultivation according to (Verduyn *et al.* 1990): glucose 15 g/L, $(NH_4)_2SO_4$ 15 g/L, KH_2PO_4 9 g/L, $MgSO_4 \times 7H_2O$ 1.5 g/L, EDTA-Na_2 45 mg/L, $ZnSO_4 \times 7H_2O$ 13.5 g/L, $MnCl_2 \times 4H_2O$ 3.0 mg/L, $CoCl_2 \times 6H_2O$ 0.9 mg/L, $CuSO_4 \times 5H_2O$ 0.9 g/L, $Na_2MoO_4 \times 2H_2O$ 1.2 mg/L, $CaCl_2 \times 2H_2O$ 13.5 mg/L, $FeSO_4 \times 7H_2O$ 9.0 mg/L, H_3BO_3 3.0mg/L, KI 0.3 mg/L, d-biotin 0.15 mg/L, Ca-D(+)pantothenate 3.0 mg/L, nicotinic acid 3.0 mg/L, myoinositol 75.0 mg/L, thiamine hydrochloride 3.0 mg/L, pyridoxal hydrochloride 3.0 mg/L, p-aminobenzoic acid 0.6 mg/L. Additionally, ergosterol (10 mg/L) and Tween 80 (420 mg/L) were dissolved in ethanol (2.84 g/L) and added to CEN.PK medium as an anaerobic supplement.

Yeasts from stock were pre-cultured aerobically on agar plates at 30°C. Some colonies were picked up and inoculated into 5 mL liquid anaerobic CEN.PK medium for overnight incubation at 30°C, usually it results in OD_{660} ~0.1 *o.u.*

Growth conditions

Pre-culture was inoculated into 300 mL of anaerobic CEN.PK medium with 15 g/L of glucose in 500 *mL* flasks. The anaerobic batch growth was performed in Aquatron® (INFORS HT, Switzerland) orbital water bath shaker (250 rpm) with gas-lid under constant nitrogen flow (~0.5 L/h) through the shaker ($pO_2 = 0\%$). The temperature control in the shaker was aided with an external refrigerated circulator (HAAKE F3 Fisons, Germany). The growth temperatures were between 5 and 40°C with ± 0.1°C accuracy within each experiment. Growth experiments were run always in duplicate (two flasks).

Biomass measure and growth parameters

At time points, samples for dry weight of biomass (C_x) and for optical density (OD_{660}) measurements were collected. For measuring of the dry biomass, 10 *mL* of the culture was sampled and immediately filtered out on pre-waited filter (0.2 μm) under vacuum. The pellet was twice washed with 10 *mL* of ice-cold 0.9% NaCl solution and dried out at 115°C overnight. Change of

dry weight of biomass was followed over time until it reaches saturation (C_x^{final}; exemplified at Fig. 2). For measuring of the optical density, 0.5 *mL* of culture was diluted up to 10 *mL* (dilution factor = 20) with 0.9% NaCl solution and the light scattering property of the solute was measured with a spectrophotometer at 660 *nm* (OD_{660}), then the obtained value of the optical density was corrected with the dilution factor.

The following growth parameters: maximum specific growth rate (μ_{max}), final dry biomass concentration reached in the batch (C_x^{final}), biomass yield on glucose ($Y_{x/glc}$) and specific rate of glucose consumption (r_{glc}) were calculated from the same growth kinetic curves (as exemplified at Fig. 2), but analyzed and published in separate publication (Zakhartsev *et al.* 2015). Nevertheless, they are reported in Table 1 since they are used in the data analysis in this research and the method of their calculation is briefly described in Supplement 2 (Supporting Information).

Flow cytometry

Yeast size and intracellular granularity were studied by flow cytometry (FACSVantage™ SE from Becton Dickinson). Yeast samples (1 *mL*) were always taken in the early exponential phase of the culture growth ($OD_{660} < 1$; as exemplified in Fig. 2) and diluted by 10^3-folds in 0.9% NaCl water solution. The diluted sample was vigorously vortexed for ~20 *sec*. The cell suspension was not sonicated, since this results in partial cell disruption. Cell count was always set to 5×10^4 cells. The primary laser (argon-ion laser 488 *nm*) was used to record the light scatter by the non-stained cells. The intensity of the signal from forward scatter channel (FSC) is proportional to the particle's size, thus the FSC signal was always calibrated prior any analysis with a calibration kit 1–15 μm (Molecular Probes; Invitrogen Cat.No. F13838) and additionally with Sphero™ Rainbow calibration particles of 3.0–3.4 and 6.0–6.4 μm (BD Bioscience; Cat.No. 556 288; Cat.No.556286).

The signal from the side scatter channel (SSC) was interpreted as being proportional to the complexity of intracellular content, therefore this is a relative index of intracellular morphological complexity. The SSC signal cannot be calibrated and therefore was kept in the original arbitrary units [*a.u.*].

Unfortunately, the flow cytometer BD FACSVantage™ SE cannot measure the sample volume in which the selected 'cells count' was measured, therefore it was not possible to calculate the cell concentration achieved in the culture. The flow cytometry data were analyzed using the supplied Becton & Dickinson FACSDiva software v. 4.2.1.

Data analysis

The two-peak size distribution histogram (exemplified at Fig. 1B.2) was interpreted as superposition of a peak of single (or (*m*)other) cells in G_1-growth phase (with diameter $\emptyset_1$ in μm) with a peak of budding (or *m*+*bud*) cells in $S/G_2/M$ growth phases (with diameter $\emptyset_2$ in μm) [for the notations visit Fig. 1A]. Correspondingly, the size of the bud was calculated as $\emptyset_{bud} = \emptyset_2 - \emptyset_1$. The linearized size distribution histograms are slightly skewed; therefore, they were fit to sum of two log(Gaussian) functions (Supplement 3, Supporting Information). The results of the fitting (accepted goodness of fit $R^2 > 0.98$) are presented at Fig. S1 (Supporting Information). The non-linear regression analysis and integration of the peak area were performed in MATLAB. The peak areas were normalized to their sum and expressed as fractions (f_i) in Table 1 and additionally depicted at Fig. S1 (Supporting Information).

The mother cell and the bud were approximated as spheres with diameters ($\emptyset_i$) measured by FC (Fig. 1A) and the approximated surface area (S_{TS}; [μm^2] or [m^2]) and the approximated total intracellular volume (V_{TV}; [μm^3] or [L_{TV}]) of an averaged cell (single mother cells and budding cells together) in population were approximated as:

$$S_{TS} = f_1 S_{TS}^m + f_2 \left(S_{TS}^m + S_{TS}^{bud}\right) = \pi \left(f_1 \emptyset_1^2 + f_2 \left(\emptyset_1^2 + \emptyset_{bud}^2\right)\right) \quad (5)$$

$$V_{TV} = f_1 V_{TV}^m + f_2 \left(V_{TV}^m + V_{TV}^{bud}\right) = \frac{\pi}{6} \left(f_1 \emptyset_1^3 + f_2 \left(\emptyset_1^3 + \emptyset_{bud}^3\right)\right) \quad (6)$$

Where: f_1—fraction of the single mother cells in G_1-growth phase; f_2—fraction of the budding cells in $S/G_2/M$-growth phases; S_{TS}^m—total approximated surface area of a single mother cells [μm^2]; S_{TS}^{bud}—total approximated surface area of a bud [μm^2]; V_{TV}^m—total approximated cell volume of a single mother cells [μm^3] or [L_{TV}]; V_{TV}^{bud}—total approximated cell volume of a bud [μm^3] or [L_{TV}]; $\emptyset_1$—averaged diameter of the single mother cells [μm]; $\emptyset_{bud}$—averaged diameter of the bud [μm]. Correspondingly, the surface-to-volume ratio of an averaged cell in population (S_{TS}/V_{TV}; [m^2/L_{TV}]) was calculated from equations (5) and (6). All measured and calculated data are reported in Table 1.

Length of budding period (t_b) in course of the exponential growth phase was calculated according to (Vanoni, Vai and Frascotti 1984; Porro *et al.* 2009) as:

$$t_b = \frac{\ln(1 + f_2)}{\mu_{max}} \quad (7)$$

Where: f_2—fraction of the budding cells in $S/G_2/M$-growth phases [-]; μ_{max}—maximum specific growth rate of biomass [h^{-1}].

Datasets at Figs 4 and 5 were fit to one-phase exponential decay function to reveal the asymptotes.

RESULTS AND DISCUSSIONS

The flow cytometry allows accurate monitoring of the optical properties of individual cells from the population. The cells of the yeast can be considered as ellipsoids with ratio among the semi-axes $a = b < c$ (Fig. 1A), consequently, geometrically they are prolate spheroids. There is superposition of two major factors that result in the normal Gaussian distribution of the cell sizes of the yeast cells in population measured by FC: (i) natural variability in geometric shapes (*e.g.* size and semi-axes ratio); (ii) spatial position of a cell in course of the measurements in the capillary of the FC. In fact, the prolate spheroidal particles enter into the measuring capillary of FC with random axial rotation angle, therefore they have different optical projection against the laser beam and consequently it results in the variability of the light scatter (*e.g.* FSC signal). Thus, the parameters of cell size distribution histogram are insufficient in order to calculate the semi-axes (*a*, *b*, *c*) of yeast cells (Fig. 1A). Consequently, as the reasonable compromise for the problem, the shape of the yeast cells has been approximated to the sphere with diameter $\emptyset_i$ (Fig. 1A). Of course, this approximation has some error, which nevertheless cannot be quantified on the basis of the FC data, and consequently the cellular volume and surface were defined as the 'approximated' throughout the research.

A typical size distribution of non-stained yeast cell population that grows under anaerobic substrate-unlimited

Table 1. Cellular parameters of yeast *Saccharomyces cerevisiae* achieved in glucose unlimited anaerobic batch cultures at different growth temperatures.

Growth temperature	Cell diameter 1[a] $\emptyset_1$	Cell diameter 2[b] $\emptyset_2$	Bud[c] diameter $\emptyset_{bud}$	SSC[d]	Fraction of cells with $\emptyset_1$	Fraction of cells with $\emptyset_2$	S_{TS}[f]	V_{TV}[g]	S_{TS}/V_{TV}[h]	μ_{max}[i]	C_x^{final}[j]	$Y_{x/s}$[k]	r_{glc}[l]	t_b[m]
[°C]	[μm]	[μm]	[μm]	[a.u.][e]	f_1	f_2	[μm^2]	[μm^3]	$[\frac{m^2}{L_{TV}}]$	$[\frac{1}{h}]$	$[\frac{g_{dw}}{L_R}]$	$[\frac{g_{dw}}{g_{glc}}]$	$[\frac{g_{glc}}{g_{dw}h}]$	[h]
5	10.20 ± 0.05	15.00 ± 0.00	4.80	2142 ± 101	0.955	0.045	330.1	558.3	591.3	0.008	1.100	0.073	0.102	5.50
10	9.02 ± 0.01	14.32 ± 0.00	5.30	1724 ± 19	0.830	0.170	270.5	397.2	680.9	0.030	1.445	0.096	0.312	5.22
15	8.75 ± 0.00	14.06 ± 0.41	5.31	1608 ± 45	0.721	0.279	265.3	372.7	711.7	0.068	1.643	0.110	0.616	3.62
18.5	8.27 ± 0.00	13.91 ± 0.00	5.63	1513 ± 5	0.673	0.327	247.7	327.3	756.9	0.115	1.918	0.128	0.898	2.46
22.5	8.15 ± 0.47	13.22 ± 0.39	5.07	1177 ± 87	0.698	0.302	232.9	303.8	766.8	0.167	1.910	0.127	1.301	1.58
26.3	8.21 ± 0.22	14.16 ± 0.14	5.95	1176 ± 22	0.702	0.298	244.8	322.5	759.1	0.250	2.108	0.141	1.780	1.04
30	8.17 ± 0.35	14.42 ± 0.38	6.25	897	0.813	0.187	232.6	309.4	751.9	0.319	2.070	0.132	2.425	0.54
31	7.84 ± 0.08	15.05 ± 0.00	7.21	773 ± 34	0.930	0.070	204.5	266.0	768.8	0.379	2.000	0.133	2.843	0.18
33	7.93 ± 0.01	13.41 ± 0.01	5.48	464 ± 9	0.923	0.077	204.9	267.8	764.9	0.309	1.590	0.106	2.917	0.24
34	7.81 ± 0.01	13.62 ± 0.23	5.81	576 ± 5	0.582	0.418	235.9	292.2	807.2	0.258	1.758	0.106	2.434	1.35
35	*n/a*	*n/a*	*n/a*	639 ± 14	*n/a*	*n/a*	*n/a*	*n/a*	*n/a*	0.242	1.520	0.102	2.376	*n/a*
37.5	7.58 ± 0.01	12.50 ± 0.00	4.92	1008 ± 22	0.690	0.310	204.0	247.2	825.2	0.195	1.358	0.091	2.159	1.39
40	7.97 ± 0.01	12.89 ± 0.00	4.92	1093 ± 54	0.438	0.562	242.2	299.9	807.6	0.111	1.018	0.068	1.623	4.02

[a] Averaged diameter of single mother cells in G_1 growth phase (Fig. 1) ($\pm$ *min/max*).
[b] Averaged diameter of budding cells in $S/G_2/M$ growth phases (Fig. 1) ($\pm$ *min/max*).
[c] Diameter of bud, $\emptyset_{bud} = \emptyset_2 - \emptyset_1$.
[d] Values of averaged Side Scatter Channel signal from the flow cytometer ($\pm$ *min/max*).
[e] Arbitrary units, was reported by flow cytometer.
[f] Approximated surface area of an averaged cell in population (equation (5)).
[g] Approximated total intracellular volume of an averaged cell in population (equation (6)).
[h] Surface-to-volume ratio.
[i] Maximum specific growth rate of biomass, was reported in Zakhartsev *et al.* (2015).
[j] Final biomass concentration achieved in anaerobic batch culture, was reported in Zakhartsev *et al.* (2015) (exemplified at Fig. 2).
[k] Biomass yield on glucose in substrate unlimited anaerobic batch, was reported in Zakhartsev *et al.* (2015).
[l] Specific rate of glucose consumption, was reported in Zakhartsev *et al.* (2015).
[m] Length of the budding period (equation (7)).
n/a—not available.

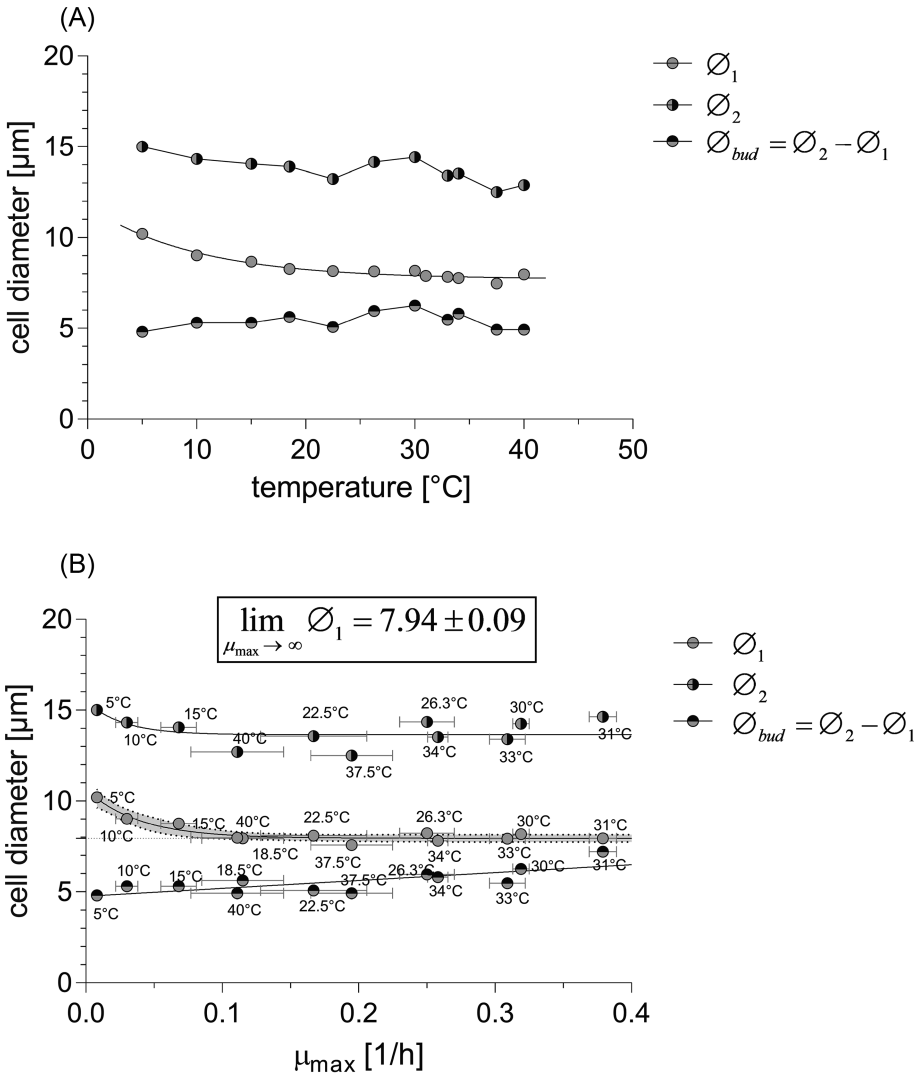

Figure 4. Dependence of averaged cell diameter of yeast *Saccharomyces cerevisiae* CEN.PK 113–7D in substrate unlimited anaerobic batch growth on (A) growth temperature and (B) on maximum specific growth rate achieved at corresponding temperature (μ_{max}, reported in Zakhartsev *et al.* 2015). The diameter of single cells ($\emptyset_1$) and the diameter of the budding cells ($\emptyset_2$) were defined at Fig. 1A, and accordingly the diameter of the bud is $\emptyset_{bud} = \emptyset_2 - \emptyset_1$. Dashed and shaded area is 95% Confidence Interval of one-phase exponential decay regression curve.

conditions (as exemplified in Fig. 2) is observed as a two-peak distribution (Fig. 1B.2), where $\emptyset_1 < \emptyset_2$. The peak with $\emptyset_1$ is formed by the fraction of single cells in G_1-growth phase in the population, whereas the peak with $\emptyset_2$ is formed by the fraction of the budding cells in $S/G_2/M$-growth phases in the population [10]. Obviously, that the budding cells have longer semi-axis *c* (Fig. 1A), which results in *a fortiori* wider width of the size distribution-peak (for more examples see Figs 3 and S1). Correspondingly, integration of the peak areas gives fractions of cells in corresponding cell cycle phases within the yeast population.

The different cellular parameters (*e.g.* cell size, granularity SSC-index, approximated surface area, total approximated intracellular volume, *etc*) of yeast cultures were monitored at different temperatures in anaerobic glucose-unlimited batch growth conditions (Table 1). Within each isothermal growth conditions, the biomass increment was followed over the time and different growth parameters of the biomass (*e.g.* maximum specific growth rate, biomass yield, specific rate of glucose consumption) were additionally determined from the same cultures (Table 1; as exemplified in Fig. 2, and the whole dataset was published in Zakhartsev *et al.* 2015).

Temperature-induced change in cellular size, volume and S_{TS}/V_{TV}

Averaged diameters of the single and the budding cells of yeast *Saccharomyces cerevisiae* CEN.PK 113–7D were measured under different isothermal growth conditions between 5 and 40°C (Table 1). The diameter of averaged single cells exponentially decays from 10.2 μm at 5°C down to asymptotic value at around 8 μm (Fig. 4A): the lower the growth temperature, the larger is the cell size. The asymptotic (or true critical) size of the single cells is more accurately determined in relationship with μ_{max} as 7.94 ± 0.09 μm (Fig. 4B). The critical size of single yeast cells growing at $T \geq 18.5$°C is invariant, whereas growth at $T < 18.5$°C leads to the gaining of the cell size. Whereas the averaged diameter of the bud linearly depends on the μ_{max} (Fig. 4B; the slope is

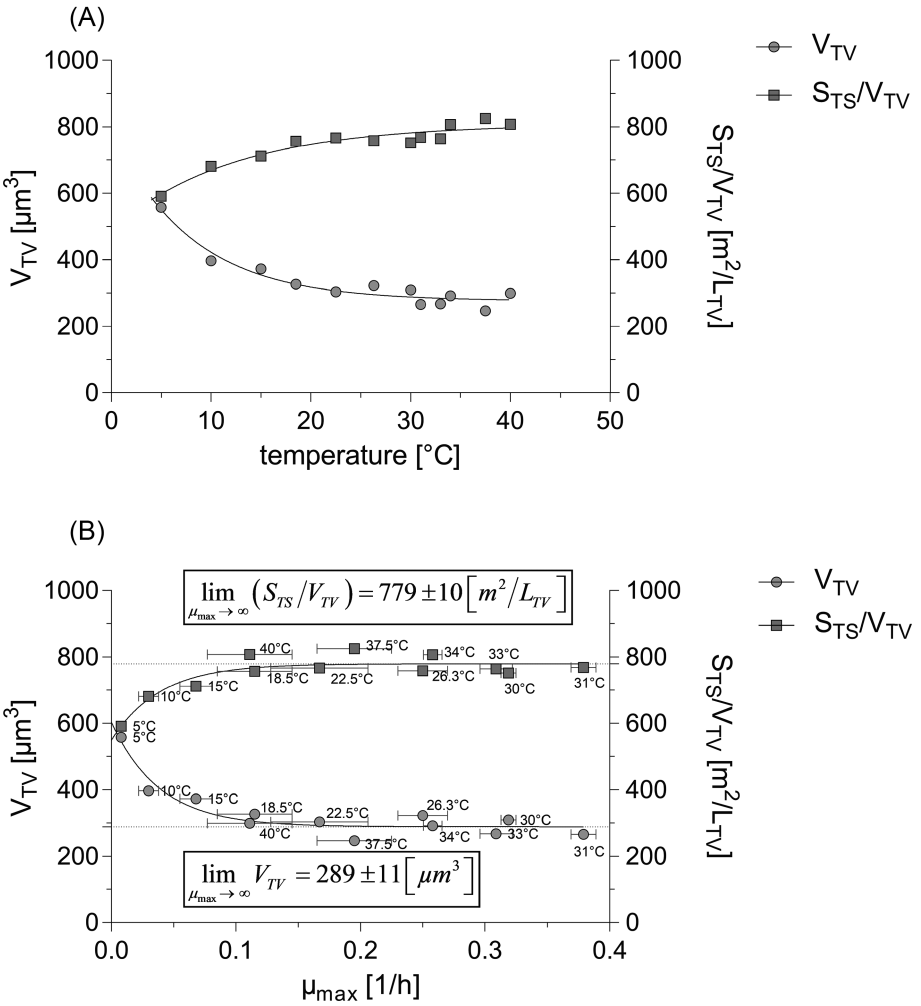

Figure 5. (i) Total approximated cell volume (V_{TV}) and (ii) surface-to-volume ratio (S_{TS}/V_{TV}) of an averaged cell of yeast *Saccharomyces cerevisiae* CEN.PK 113–7D in substrate unlimited anaerobic batch growth in dependence on (A) growth temperature and (B) maximum specific growth rate. Calculated value of V_{TV} and S_{TS}/V_{TV} take in account fractional composition of the cell population (equations (5) and (6)) at given growth conditions (Table 1, Fig. S1, Supporting Information). Within 18.5–40°C temperature range, the values of V_{TV} and S_{TS}/V_{TV} do not deviate from their corresponding asymptotic values, while exponentially deviate at temperatures below 18.5°C.

significantly non-zero ($F = 13.84$, $P = 0.004$)), thus: the faster μ_{max}, the larger is the bud diameter. The size of the bud varies from 50% (at 5°C) up to 90% (at 31°C) of the size of the mother cell. Nevertheless, on average, the bud diameter is $\tilde{\emptyset}_{bud} = 0.67 \cdot \emptyset_1 \pm 0.11$, although there is no direct correlation between bud's and mother's diameters (Fig. 4B).

The average cellular size (Fig. 4) and consequently the approximated cellular volume of a single cell almost do not vary at growth temperatures between 18.5 and 40°C (at $\mu_{max} > 0.1\ h^{-1}$), whereas below 18.5°C (at $\mu_{max} < 0.1\ h^{-1}$), the temperature effect is clearly profound and cells become large. Thus, 7.94 μm is the asymptotic true critical cellular diameter of a single cell which is required to pass through the G_1-checkpoint and start budding under any temperatures above 18.5°C. However, at temperatures below 18.5°C ($\mu_{max} < 0.1\ h^{-1}$), the cells are likely retained longer time in G_1-growth phase where they keep on growing until they perhaps fulfill another passage-criterion (*e.g.* protein or carbohydrate concentrations, *etc*) to pass this checkpoint. This conclusion is also strongly supported by the corresponding decrease of the fraction of the budding cells in the population at growth temperatures <18.5°C (Table 1, Fig. 8). It means that at low growth rates ($\mu_{max} < 0.1\ h^{-1}$) observed at temperatures <18.5°C lesser amount of cells start budding, so they perhaps either (i) are arrested in the G_1-checkpoint where they keep on growing until fulfilment of another passage-criterion or (ii) they exit from the cell cycle into G_0-phase (Boender *et al.* 2011).

Detected relationship among sizes of the single cell and the bud (Fig. 4B) resembles conclusion derived in Porro *et al.* (2009): the poor media yields a high level of asymmetry with large parent cells and very small daughter cells, whereas, in the rich media, parent and daughter cells are very close in sizes. Thus, growth temperatures <18.5°C causes similar effects as the poor growth media which limits cell growth via depletion of nutrients (*e.g.* nitrogen) supply.

The total approximated intracellular volume (V_{TV}) and approximated surface-to-volume ratio (S_{TS}/V_{TV}) of an averaged cell in population were calculated for the averaged yeast cell as the function of the growth temperature and the specific growth rate (Fig. 5). The calculation has taken in account the fractional

composition (single f_1 and budding f_2 cells) of the population at given growth conditions (equations (5) and (6), Table 1; Fig. S1, Supporting Information). Similar to averaged diameter of a single cell (Fig. 4), both of these parameters have exhibited asymptotic values ($V_{TV} = 289 \pm 11\ \mu m^3$; $S_{TS}/V_{TV} = 779 \pm 10\ m^2/L_{TV}$) at growth temperatures between 18.5 and 40°C (Fig. 5). However, at the growth temperatures <18.5°C, the averaged cellular volume increases, and at 5°C it is as much as twice higher relative to the asymptotic value. Correspondingly, the S_{TS}/V_{TV} decreases by 0.75-folds (Fig. 5).

Temperature-induced change in cellular morphology and biomass density

Monitoring of an optical density of a cell suspension at 660 *nm* (OD_{660}) is used in biotechnology as an express method to estimate the biomass content (Hulst 1957; Koch 1994). Technically speaking, measuring of the optical density of the cell suspension, in fact, is the measure of the light scattering, *i.e.* turbidity. There are several major factors which simultaneously contribute to the level of turbidity exerted by the cell suspension: (i) cell concentration (N), (ii) cell size and shape ($\emptyset$) and (iii) cell opacity and complexity of internal content (*i.e.* granularity or other morphological complexity) (equation (2)) (Hulst 1957; Koch 1994). Under invariant growth conditions, when the cell size and opacity can be assumed to be constant, the OD_{660} becomes directly proportional to the cell concentration only and consequently can be related to the dry biomass concentration after calibration (Burke, Dawson and Stearns 2000). The wavelength of 660 *nm* is often used in common laboratory practice because there are no endogenous chromophores in microbes that absorb the light of this wavelength. Nevertheless, the individual contribution of each factor to the value of OD_{660} cannot be segregated and therefore the OD_{660} value has to be treated as the integral value.

At every growth temperature the OD_{660} was measured along with the final concentration of the dry biomass (C_x^{final}; Figs 2 and 6A). As expected, there is a linear relationship between them. However, there are two distinctive temperature regions (5–26.3°C *vs.* 30–40°C) where this relationship significantly differs with step-wise shift at 26.3–30°C. Due to integrative nature of the OD_{660} value, it is impossible to relate observed step-wise shift to any specific contributors (*e.g.* N, $\emptyset$, cell opacity). Nevertheless, the temperature-induced changes of the cell size can be excluded as the potential contributor to the acute shift of the parameters at these growth temperatures, since the critical cellular size is invariant at temperatures above 18.5°C (Figs 4 and 5).

Alternatively, the FC is suitable technology that allows simultaneous multiparametric analysis of a cell suspension with or without employing fluorescent probes/labels. The FC of non-stained cell population allows estimating cell size (by forward scatter of the laser beam, further abbreviated as FSC) and morphological complexity (by side scatter of the laser beam, further abbreviated as SSC) (Fig. 1B) and therefore distinguishing the cell types. However, employing of the fluorescent labels (both endogenous and exogenous being specifically attached to biomarkers) enormously expands the list of measured parameters [*e.g.* cell pigmentation, total DNA/RNA content, cell cycle analysis, cell kinetics, proliferation, chromosome analysis, detection of variously labeled biomarkers, *etc*].

With the aid of FC, it becomes possible to semi-quantitatively estimate the morphological variation of the individual yeast cells. The magnitude of the SSC signal obtained from the FC (Fig. 1B.3) exclusively depends on the inner morphological complexity of a cell (*i.e.* carbohydrate deposits in form of granules per cell volume, shape and size of the nucleus, amount and type of cytoplasmic organelles like mitochondria, vacuole, peroxisomes, cytoplasmic and membrane-associated ribosomes per cell volume, *etc*), *i.e.* so-called intracellular granularity. So, the SSC depends neither on the cellular size ($\emptyset$) nor on the cell concentration (N), since it is measured as the side scatter of the light of the individual cells. Thus, the granularity, expressed as the SSC signal, is an integral parameter that exclusively includes both qualitative and quantitative aspects of the intracellular content; thus, the higher cytoplasm granularity, the stronger is side scatter of the laser beam. However, without aid of specialized fluorescent labels it is impossible to distinguish individual contributions from different cytoplasmic constituents (*e.g.* mitochondria, ribosomes, glycogen granules, *etc*). Yeast growth at different temperatures reveals variation of the cellular granularity (Fig. 6B). The maximal SSC value was observed at 5°C, whereas the minimal value at 33°C, and then again it increases towards 40°C (Fig. 6B). Consequently, the question arises: what is a possible reason for temperature induced variation of intracellular granularity?

Plotting the SSC-index against OD_{660} reveals linear relationship which is distinctively different in two temperature regions (5–31°C *vs.* 33–40°C; Fig. 6C). Since SSC-index exclusively describes the internal complexity and does not depend neither on $\emptyset$ nor on N, then the observed shift in the relationship is completely defined by the acute shift in the cellular morphology, *i.e.* temperature induced change in the internal cytoplasmic complexity of the yeast cells.

From the chemostat experiment, it is well documented, that the macromolecular composition of the microbial biomass linearly depends on the specific growth rate (*i.e.* μ_{max}) (Nissen *et al.* 1997; Lange and Heijnen 2001). Particularly, carbohydrate content in the yeast *Saccharomyces cerevisiae* biomass decreases with increase of μ_{max}: maximal content (up to 50% of the dry biomass) is observed at slow μ_{max}, whereas minimal content (down to 15% of the dry biomass) is at fast μ_{max} (Lange and Heijnen 2001). Therefore, it is logic to check whether SSC-index is related to intensity of the glucose metabolism.

Plotting the SSC-index against specific rate of glucose consumption (r_{glc}) reveals very tight exponential relationship between these variables (Fig. 6D). High carbohydrate or polysaccharide content in yeast *Saccharomyces cerevisiae* cells can be deposited in form of cytoplasmic glycogen granules (Coulary, Aigle and Schaeffer 2001; Boender *et al.* 2011), which apparently contribute to the final value of the intracellular granularity. Glycogen accumulation in cytoplasm is a dynamic process, because it is a balance-process between rates of glycogen synthesis and its consumption. From the other side, it is obvious from Fig. 6D that the rate of the glucose consumption causes the effect on the intracellular granularity: the faster is r_{glc}, the lower is the intracellular granularity. At low μ_{max} (which is accompanied by the low r_{glc}; Zakhartsev *et al.* 2015), deposition of glucose into glycogen prevents glucose from immediate entering into glycolysis, which allows accumulating of carbon and energy to be used later in course of the budding period (Coulary, Aigle and Schaeffer 2001). Consequently, the carbohydrate content increases as the biomass constituent at low μ_{max} (Lange and Heijnen 2001) and it is expected that correspondingly intracellular granularity increases accordingly (Fig. 6D). Nevertheless, since the SSC-index is the integrative value, then it is impossible (at least based on this data) to distinguish input of the

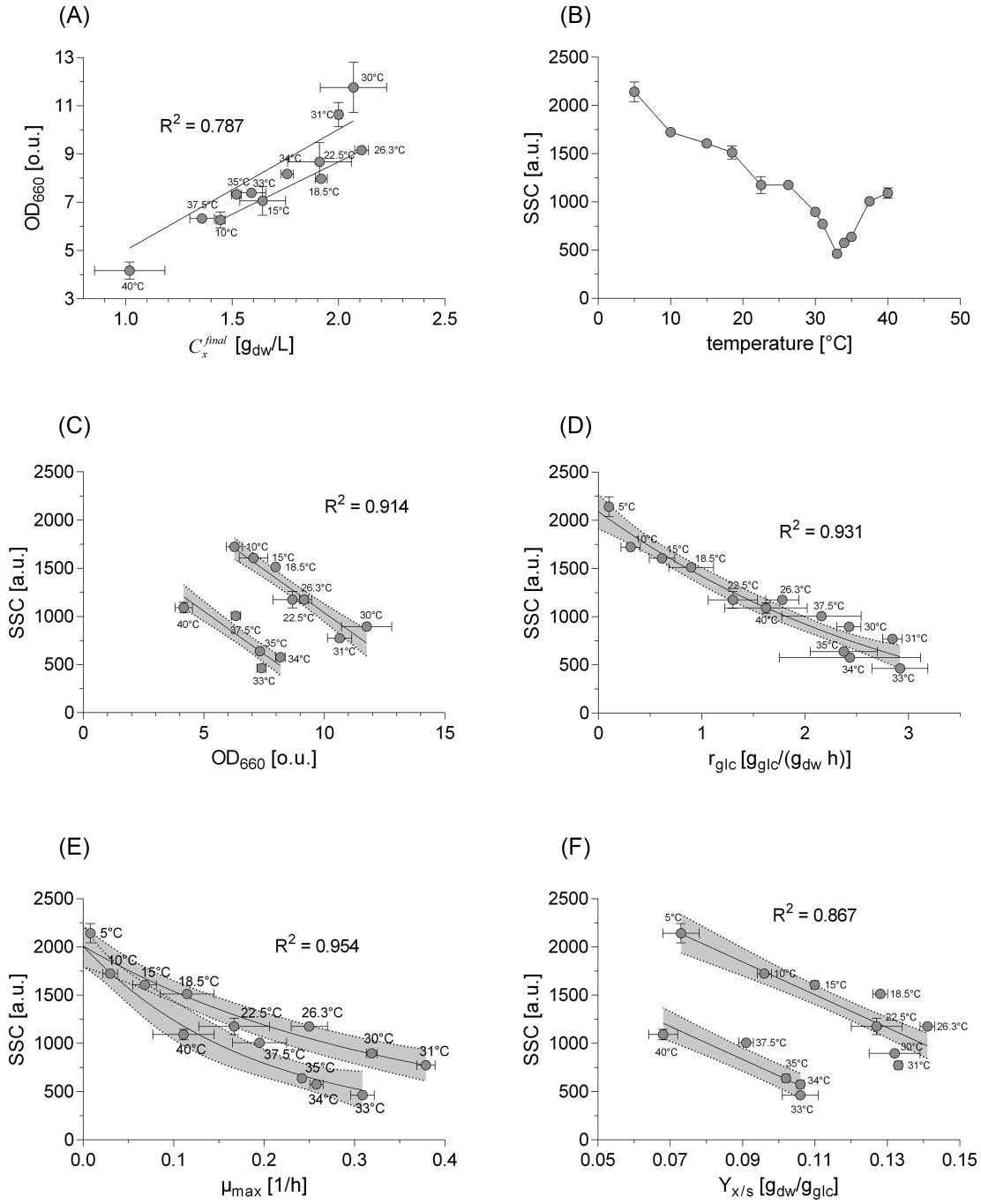

Figure 6. Temperature-induced change in cellular morphology (*e.g.* SSC-index) of yeast *Saccharomyces cerevisiae* CEN.PK 113–7D in anaerobic glucose-unlimited batch growth. (A) Relationship between the final concentration of the dry biomass achieved in the batch (C_x^{final}; see Fig. 2 for the notations) and the light scattering properties of the cell suspension at 660 *nm* (OD_{660}). There is significant difference between slopes (F = 15.15; DFn = 1, DFn = 22, P = 0.0008) of two temperature regions (10–26.3°C *vs.* 30–40°C). Dependence of averaged cellular granularity index (SSC) on: (B) the growth temperature; (C) OD_{660} (two lines; F = 1.034; DFn = 1, DFn = 18, P = 0.3226); (D) specific glucose uptake rate (one curve for both data sets; F = 1.558; DFn = 3, DFn = 19, P = 0.2323); (E) maximum specific growth rate (two curves for both data sets); (F) the biomass yield on glucose (two lines; F = 0.1682; DFn = 1, DFn = 22, P = 0.6857). Dashed and shaded areas are 95% Confidence Intervals for corresponding regression curves.

glycogen granules from inputs of other unaccounted contributors (*e.g.* amounts of ribosomes, mitochondria; Farewell and Neidhardt (1998)).

As it was shown previously (Zakhartsev *et al.* 2015), there are two temperature regions (5–31°C *vs.* 33–40°C) for yeast *Saccharomyces cerevisiae* CEN.PK 113–7D where r_{glc} differently depends on μ_{max}, and observed difference is due to 12-folds increased maintenance rate in temperature region 33–40°C *versus* 5–31°C. Plotting of the SSC-index against μ_{max} also reveals similar temperature regions (5–31°C *vs.* 33–40°C) (Fig. 6E). In general, the faster cells grow, the less granulated they are. Nevertheless, the SSC-index is significantly getting lower in the

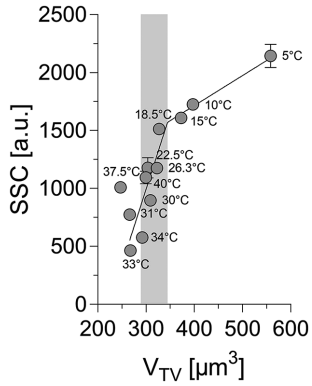

Figure 7. The relationship between averaged cell granularity (*i.e.* SSC-index) and total approximated cell volume of an averaged cell of yeast *Saccharomyces cerevisiae* CEN.PK 113–7D grown at different temperatures in glucose unlimited batch cultures. The shaded area indicates the intracellular volume region between asymptotic 289 μm^3 (Fig. 5B) and 344 μm^3 as the break-point of the two-phase regression line. The two-phase regression analysis has revealed, that almost 3-folds variation of cellular granularity within $18^\circ C < T < 40^\circ C$ is not accompanied by the same degree of variability in total approximated cell volume of an averaged cell in population V_{TV} ($r = 0.807$, $R^2 = 0.652$, $P = 0.008$), whereas at $T < 15^\circ C$, the change in one parameter causes adequate change in the other ($r = 0.999$, $R^2 = 0.999$, $P = 0.0006$).

temperature region 33–40°C where the cellular rate of maintenance is increased 12-folds (Zakhartsev *et al.* 2015). The maintenance processes consume ATP without corresponding formation of a new biomass. Therefore, there is corresponding relative increase in glucose consumption rate in 33–40°C to provide extra energy for the increased rate of maintenance, which is supported by lowered SSC-index if we assume low granularity as a lack of energy related deposits (Fig. 6E). This observation is in agreement with Fig. 6D: faster r_{glc} gives lower SSC-index. The existence of two distinctive temperature regions (5–31°C *vs.* 33–40°C) in cellular morphology becomes even more obvious when SSC-index is plotted against of the biomass yield on glucose (Fig. 6F). If to compare the same values of the biomass yields achieved in both temperature regions, then it is obvious that the cells from 33–40°C region have significantly lower granularity (Fig. 6F). This can be explained that in this temperature region, the larger fraction of glucose is metabolized to the end-products (*e.g.* ethanol, CO_2, *etc*) to form extra ATP as it is required by increased maintenance rate. Thus, the lowered intracellular granularity in 33–40°C reflects higher turnover in energy metabolism fed by glucose due to increased maintenance rate under similar biomass yields. The relationship between specific rate of glucose consumption, specific growth rate of biomass and energy metabolism under different growth temperatures was considered in details in Zakhartsev *et al.* (2015); hereby, we would like to add that the early observed metabolic adjustments achieved in course of the temperature dependent growth are accompanied by independently observed changes in the intracellular morphology, which are somehow related to the energy metabolism. Thus, the biomass which has been formed under 33–40°C growth temperatures is morphologically different.

As we have observed in our experiments, the granularity significantly varies relative to the average approximated cell volume (Fig. 7). In fact, between 18.5°C and 40°C, the SSC can vary up to 3-folds within the relatively small variation of the average approximated cell volume (~15%). Although, under $\mu_{max} < 0.1\ h^{-1}$ (that are induced by growth temperature <18.5°C), the increase of the cellular volume is adequately accompanied with increase of the intracellular granularity. If we consider an increasing intracellular granularity as a consequence of increasing amounts of glycogen granules or other intracellular structures, then at relatively constant cell volume V_{TV} this variability should result in change of the density of the biomass packing, *i.e.* ρ_x. Consequently, it is expected that density of the biomass packing should vary in dependence of the growth conditions. However, in order to assess this hypothesis, the accurate measure of the cell concentration (N) is required along with direct measures of C_x and V_{TV} (equation (2)) under different growth conditions. Unfortunately, the flow cytometer BD FACSVantage™ SE cannot measure the cell concentration in the collected samples, therefore it was not possible to calculate ρ_x.

As a sum: step-wise increase of maintenance rate (which has been observed in 33–40°C growth temperatures; Zakhartsev *et al.* 2015) is accompanied by a relative increase of glucose consumption rate and also with a significant morphological shift in the intracellular structures, which potentially lead to the reduction of the biomass density. Based on our data, we only can speculate about the causes which change the integrative intracellular granularity, since we cannot distinguish the exact contribution of different factors.

Temperature-induced change in fraction of budding cells

Growth temperature has the profound effect on the specific growth rate of the biomass of yeast (Zakhartsev *et al.* 2015) through affecting the duration of the cell cycle (Vanoni, Vai and Frascotti 1984): the lower temperature, the slower is the cell cycle and therefore the longer doubling time of the biomass (equation (4), Fig. 3). Essentially, a doubling of the microbial biomass reflects a process of division of cells in half and further their growth in terms of volume and mass. In the case of yeasts *Saccharomyces cerevisiae*, cells are dividing by means of budding and the formed cells are asymmetric in size: larger mother cell and smaller daughter cell (Figs 1 and 4). The degree of asymmetry is a variable, which depends on different factors (Porro *et al.* 2009). For example, reduction in the growth rate due to nitrogen limitations in feed results in larger mother cells and smaller daughter cells (Porro *et al.* 2009). However, as we observe, a similar effect is induced by the growth temperature as well (Fig. 4B).

Additionally, the structure of the population of the exponentially growing batch culture also varies in dependence of the growth temperature (Fig. S1, Supporting Information). Particularly, the fraction of the budding cells (f_2; fraction of cells with $\emptyset_2$ denoted at Fig. 1) clearly depends on the growth temperature (Fig. 8). The f_2 gradually increases from 0.045 at 5°C up to 0.32 at 18.5°C, then again gradually decreases down to 0.07 at 31–33°C, and then acutely rises up to 0.56 at 40°C (Fig. 8). Correspondingly, a question arises: what could be the reasons for such effect?

The length of the budding period (t_b, equation (7)) has been calculated on the base of independently measured μ_{max} (Zakhartsev *et al.* 2015) and f_2 (Table 1). As expected, t_b mainly depends on μ_{max} (Fig. 8C). The shortest t_b was observed at the fastest μ_{max} at 31–33°C (Fig. 8) and numerical values of t_b observed in this research are in the line with the early published results (Vanoni, Vai and Frascotti 1984; Porro *et al.* 2009).

The phases of the cell cycle are separated by checkpoints (Fig. 3). There are two major checkpoints in yeast cell cycle: (i) G_1 or so-called Start and (ii) spindle assembly or so-called Finish (Chen *et al.* 2004). Yeast cells can be arrested in

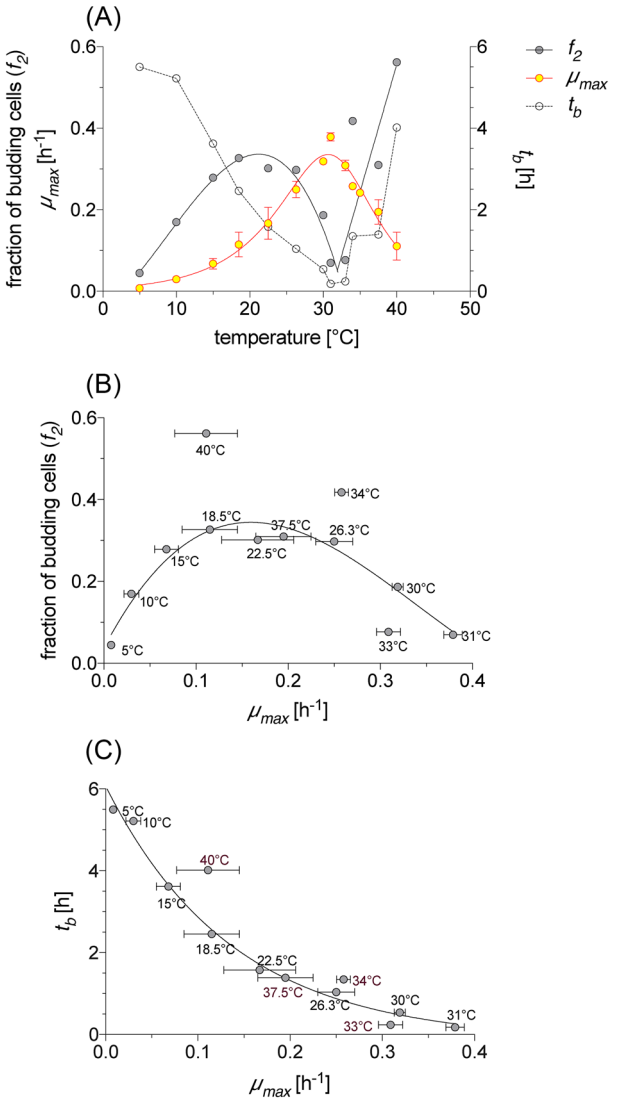

Figure 8. Fraction of budding cells (in $S/G_2/M$ phases with $\emptyset_2$; defined at Fig. 1) within the cell population and duration of budding period (t_b; equation (7)) in dependence on (A) growth temperature and (B,C) maximum specific growth rate of the biomass (μ_{max}) in anaerobic glucose unlimited batch cultures of yeast *Saccharomyces cerevisiae* CEN.PK 113–7D. In (B,C), the data points between 33°C and 40°C were not used for fitting.

either checkpoint until the fulfillment of the passing criteria. At G_1-checkpoint, a cell can be arrested if DNA damage is detected, mating pheromone is present, presence of specific gene products, the lack of protein levels or the cell has not reached the critical cell size (*i.e.* V_{TV}), then it is unable to undergo the Start transition which commits the cell to a new round of DNA synthesis and mitosis, e.g. budding (Vanoni, Vai and Frascotti 1984). Thereby, if the μ_{max} reduction is accompanied by increasing fraction of the non-budding cells in the population then it may indicate the fact that cells cannot pass through the G_1-checkpoint until they fulfill mentioned above criteria. Thus, reaching the critical cellular size and protein content are among the important requirements to come through the G_1-checkpoint in the cell cycle (Hartwell 1974). From the other side, at spindle assembly checkpoint, a cell can be arrested in metaphase if DNA damage is detected, DNA is not replicated completely, or chromosomes are not aligned on the metaphase plate, then it is unable to undergo the transition of the Finish checkpoint, thus sister chromatids remain unseparated and consequently the cytokinesis is not fulfilled. Thus, if the μ_{max} reduction is accompanied by increasing fraction of the budding cells in the population then it may indicate cell arrest in the Finish checkpoint (for references see Fig. 3).

In general, it can be roughly approximated that the $S/G_2/M$-phase is responsible for the propagation of *N* through the cell cycle, whereas the G_1-phase is responsible for the propagation of the weight/mass of the biomass through the cellular growth (Fig. 3). The yeast cell cycle can be considered under following assumptions (Fig. 3): a single cell enlarges in volume only during G_1-phase and as soon as it reaches the critical size and fulfills other passage-criteria (*e.g.* carbohydrate deposit, protein concentration, *etc.*) it passes G_1-checkpoint in the cell cycle and starts budding (Porro *et al.* 2009). The duration of the G_1-phase can strongly vary, which is definitely reflected on the specific growth rate (μ_{max}). It is known that the increase in G_1-phase duration is accompanied by a strong increase in the levels of the reserved carbohydrate. These carbohydrates are metabolized again before the emergence of the bud, implying a transient increase in ATP flux which is required for progression through the cell cycle (Sillje *et al.* 1997). After cell division, the larger mother cell can enter S-phase after accumulation of sufficient reserves, while the daughter cell additionally has to grow first to reach volume required for the budding (Sillje *et al.* 1997). A cell gains the mass only in course of the G_1-phase, due to substrate consumption, its assimilation into biomass, including the formation deposits (carbohydrates, polyphosphates, *etc.*). During the process of the budding, the growth occurs exclusively in the bud, while the mother cell does not change in size. The budding cell is not feeding and the material growth of the bud occurs at the expenses of deposits, which are the only source of primary elements and energy in this period, *i.e.* the mass redistributes within the budding cell (Fig. 3).

Thus, if to combine all experimental data from this research with the assumptions of the yeast cell cycle, then it follows that at the population level:

i. at temperatures below 18.5°C, due to low metabolic activity, cells longer accumulate carbohydrates up to the amount required to pass the G_1-checkpoint in the cell cycle and then slower consume it in the course of the budding to form a bud of smaller size (Fig. 4B). This is confirmed by very high SSC-index (Fig. 6), meaning that it is likely that the carbohydrate deposition is getting higher (Lange and Heijnen 2001). The strong increase of intracellular granularity is accompanied by an increase of the cellular volume (Fig. 7), therefore there should not be over-densification of the packing of the cytoplasmic content. The budding activity in the population is low (*i.e.* f_2 is low; Fig. 8), because the majority of cells in the population are the single cells which are arrested at G_1-checkpoint (or may be some cells even can be in G_0-phase (Boender *et al.* 2011) at extremely low μ_{max}), therefore they keep on growing until passage through the G_1-checkpoint. Consequently, the population has a wide range of sizes and increased average approximated cellular volumes (Figs 4 and 5; Fig S1, Supporting Information). Thus, together with the prolonged $S/G_2/M$-phase (*i.e.* t_b), all these leads to the slow μ_{max} (<0.1 h^{-1}; Fig. 8). Most of the time during the cell cycle, the cells are in G_1-phase with very slow μ_{max}, additionally, low biomass yield on glucose (Table 1) is observed as well.

ii. at temperatures 18.5–26.3°C, the budding activity (f_2) is relatively high (Fig. 8) and this is accompanied by the highest biomass yield on glucose (Table 1) and moderate μ_{max} (0.1–0.25 h^{-1}) (Table 1, Fig. 8).
iii. at temperatures between 26.3°C and 31°C, the budding activity (f_2) decreases (Fig. 8) perhaps due to shortening t_b and quicker passage through the FINISH checkpoint (Fig. 3). Intracellular granularity (SSC-index) drops to the minimum, which might correspond to the reduction of the carbohydrate deposits (Lange and Heijnen 2001). Under this conditions cells are dividing very fast, and rapidly reach the critical volume, but filling of them with the intracellular content is behindhand. This is reflected in the highest metabolic activity ($0.25 < \mu_{max} < 0.35\ h^{-1}$) and slightly reduced biomass yield on substrate (Table 1). The bud reaches the maximal size and it is up to 90% of the size of the mother cell.
iv. at supraoptimal temperatures, *i.e.* above 31°C, the fraction of budding cells (f_2) acutely rises (Fig. 8) perhaps due to more often arrests in the FINISH checkpoint (Fig. 3), correspondingly t_b elongates (Fig. 8), correspondingly μ_{max} drops. Additionally, formation of cell aggregates and abnormal cell shapes (exemplified in Fig. S2, Supporting Information) contribute to the increased f_2 due to having large projection of the laser beam. This is clearly supported by the cell size distribution histograms at Fig. S1 (Supporting Information) for 37.5°C and 40°C, where the width of the f_2-peak is much broader, which is very likely is the result of the cell aggregations. The cell flocculation/aggregation was not observed by optical microscopy at temperatures below 31°C. In the temperature region 33–40°C, the rate of maintenance increases 12-folds (Zakhartsev *et al.* 2015), which results in extra glucose consumption and corresponding drop in the biomass yield (Table 1), which is additionally accompanied by the substantial shift in the cellular morphology (Fig. 6). Mostly the cells are arrested in the budding phase or aggregated, therefore the μ_{max} acutely drops.

CONCLUSIONS AND PERSPECTIVE

It was shown that the diameter of the single cells is invariant (7.94 μm) in the growth temperatures between 18.5°C and 40°C, but exponentially increases up to 10.2 μm below 18.5°C towards 5°C. Whereas, the diameter of the bud linearly varies with μ_{max}, from 50% at 5°C up to 90% at 31°C of the diameter of the single cells. Thus, the total averaged intracellular volume of a cell in population depends on both cell size and the fractional ratio between single and budding cells within the population, and it is 289 μm^3 for any growth temperatures >18.5°C, but increases up to almost 550 μm^3 at 5°C.

Analysis of intracellular morphology has revealed that the index of intracellular granularity (SSC-index) is likely related to the rate of glucose metabolism: the faster is the specific glucose consumption rate, the lower is the SSC-index. There are two temperature regions (5–31°C *vs.* 33–40°C) where the relationship between intracellular morphology and growth performance is significantly different. The possible causes of the difference have been attributed to the acute increase in the maintenance rate in the supraoptimal temperature region (*i.e.* 33–40°C).

It was shown that the temperature dependent passage through the checkpoints in the cell cycle also contributes to the effect of temperature on the μ_{max}, which is followed from the temperature induced variations in the structure of the yeast cell population.

The accurate measurement of the cell concentration (N, $[n/L_R]$) at different growth temperatures is required for the accurate calculations of the cellular density (ρ_x, $[g_{dw}/L_{TV}]$), which we could not achieve in our research. We hypothesize that ρ_x can vary with the growth temperature, but this must be experimentally proved. There is expectation of a reciprocal relationship between N and ρ_x in their contribution to the overall biomass concentration $[g_{dw}/L_R]$: the same biomass concentration can be achieved either by larger number of light-weight cells or lower number of heavier cells.

SUPPLEMENTARY DATA

Supplementary data are available at *FEMSYR* online.

ACKNOWLEDGEMENTS

The experimental part of the research has been carried out in Institute of Biochemical Engineering (IBVT, University of Stuttgart, Germany) and has been funded by the transnational research initiative 'Systems Biology of Microorganisms (SysMO)' within network MOSES: 'MicroOrganism Systems Biology: Energy and Saccharomyces cerevisiae' [http://www.sysmo.net]. Additionally, the author would like to thank Prof.Peter Scheurich (Institute of Cell Biology and Immunology, University of Stuttgart, Germany) for the experimental support, Achim Hauck (IBVT, University of Stuttgart, Germany) and Dr.Xuelian Yang (Beijing Engineering and Technology Research Center of Food Additives, Beijing Technology & Business University, Beijing, China) for the research assistance, Dr.Pavlo Holenya (Institute of Pharmacy and Molecular Biotechnology, University of Heidelberg, Germany) for the discussion of the results.

Definitions, Abbreviations, Variables and Parameters

Definitions accepted in this article:

batch culture—substrate unlimited batch growth of a culture at quasi-steady-state conditions with μ_{max} in constant volume in minimal medium with glucose as a sole carbon and energy source

granularity—the relative arbitrary value (measured by side scatter (SSC) laser light) used in flow cytometry to index an intracellular morphological complexity (*i.e.* carbohydrate deposits in form of granules per cell volume, shape and size of the nucleus, amount and type of cytoplasmic organelles like mitochondria, vacuole, peroxisomes, cytoplasmic and membrane-associated ribosomes per cell volume, membrane roughness, *etc*)

growth temperature—isothermal temperature regime during that the batch yeast culture grows

maintenance—any metabolic processes that require energy (and consequently substrate), but not leading to net formation of any new biomass. Typical examples of maintenance processes are (i) maintenance of gradients and electrical potential, (ii) futile cycles, (iii) turnover of macromolecules (*e.g.* RNA, proteins)

supraoptimal temperatures—a range of growth temperatures for microorganisms which are above the optimal temperature for growth, unlike suboptimal temperatures that are below the optimal temperature

Conflicts of interest. None declared.

Symbols:	
FC	– flow cytometry
x	– biomass
T	– temperature [°C]
t	– time [h]
Units:	
h	– hours
g_{dw}	– gram of the dry weight of biomass
g_{glc}	– gram of glucose
L_R	– liter of the reaction volume
L_{TV}	– liter of the total intracellular volume
mol	– mole of a metabolite
m^2	– square meter
$a.u.$	– arbitrary units
$o.u.$	– optical units
Quantities:	
$\mu_{\max}$	– maximum specific growth rate of dry biomass [$g_{dw}/(g_{dw} \times h)$] or [h^{-1}]
r	– specific rate of reaction [$mol/(g_{dw} \times h)$] or [$g/(g_{dw} \times h)$]
J	– metabolic flux [$mol/(L_{CV} \times h)$] or [$mol/(m^2 \times h)$]
$\emptyset_i$	– diameter of a cell measured by FC [μm] ($i = 1, 2$; 1-single cell, 2-budding cell)
S_{TS}	– total approximated surface area of an averaged cell [μm^2] or [m^2]
S_{TS}^m	– total approximated surface area of a single mother cell [μm^2] or [m^2]
S_{TS}^{bud}	– total approximated surface area of a bud [μm^2] or [m^2]
V_{TV}	– total approximated cell volume of an averaged cell [L_{TV}]
V_{TV}^m	– total approximated cell volume of a single mother cell [μm^3] or [L_{TV}]
V_{TV}^{bud}	– total approximated cell volume of a bud [μm^3] or [L_{TV}]
V_R	– reaction volume [L_R]
N	– cell concentration [n/L_R]
ρ_x	– averaged density of a biomass [g_{dw}/L_{TV}]
S_{TS}/V_{TV}	– surface-to-volume ratio of an averaged cell in population [m^2/L_{TV}]
C_x^{final}	– final dry biomass reached in glucose unlimited batch culture [g_{dw}/L_R]
OD_{660}	– optical density (or light scattering property) of the cell suspension measured at λ_{660} [$o.u.$]
t_d	– length of doubling period [h]
t_g	– length of growth period [h]
t_b	– length of budding period [h]
$Y_{x/s}$	– biomass yield on glucose in substrate unlimited batch growth [g_{dw}/g_{glc}]

REFERENCES

Boender LGM, van Maris AJA, de Hulster EAF *et al*. Cellular responses of *Saccharomyces cerevisiae* at near-zero growth rates: transcriptome analysis of anaerobic retentostat cultures. *FEMS Yeast Res* 2011;**11**:603–20.

Burke D, Dawson D, Stearns T. Measuring yeast cell density by spectrophotometer. in *Methods in yeast genetics (A Cold Spring Harbor Laboratory Course Manual)*. A Cold Spring Harbor Laboratory, 2000, 143–4.

Chen KC, Calzone L, Csikasz-Nagy A *et al*. Integrative analysis of cell cycle control in budding yeast. *MBoC* 2004;**15**:3841–62.

Coulary B, Aigle M, Schaeffer J. Evidence for glycogen structures associated with plasma membrane invaginations as visualized by freeze-substitution and the Thiery reaction in *Saccharomyces cerevisiae*. *J Electron Microsc* 2001;**50**:133–7.

Farewell A, Neidhardt FC. Effect of temperature on in vivo protein synthetic capacity in Escherichia coli. *J Bacteriol* 1998;**180**:4704–10.

Hartwell L. *Saccharomyces cerevisiae* cell cycle. *Bacteriol Rev* 1974;**38**:164–98.

Hulst VD. *Light Scattering by Small Particles*. New York: Dover Publications, 1957.

Koch AL. Growth measurement. In *Methods for General and Molecular Bacteriology*, Gerhardt P, Murray GE, Wood WA *et al*., (eds), Washington, DC: American Society for Microbiology, 1994, 248–77

Lange HC, Heijnen JJ. Statistical reconciliation of the elemental and molecular biomass composition of *Saccharomyces cerevisiae*. *Biotechnol Bioeng* 2001;**75**:334–44.

Nielsen J, Villadsen J, Liden G. *Bioreaction Engineernig Principles*. New York: Kluwer Academic/Plenum Publishers, 2003.

Nissen TL, Schulze U, Nielsen J *et al*. Flux distributions in anaerobic, glucose-limited continuous cultures of *Saccharomyces cerevisiae*. *Microbiology* 1997;**143**:203–18.

Piper P. Induction of heat shock proteins and thermotolerance. In *Yeast Protocols*, Evans IH, (ed), Totowa, New Jersey: Humana Press, 1996, 313–7.

Porro D, Vai M, Vanoni M *et al.* Analysis and modeling of growing budding yeast populations at the single cell level. *Cytometry* 2009;**75A**:114–20.

Reich JG, Selkov EE. *Energy Metabolism of the Cell*. London: Academic Press Inc., 1981.

Roels JA. *Energetics and Kinetics in Biotechnology*. Amsterdam: Elsevier Biomedical Press, 1983.

Salvado Z, Arroyo-Lopez FN, Guillamon JM *et al.* Temperature adaptation markedly determines evolution within the genus *Saccharomyces*. *Appl Environ Microbiol* 2011;**77**:2292–302.

Sillje HH, ter Schure EG, Rommens AJ *et al.* Effects of different carbon fluxes on G1 phase duration, cyclin expression, and reserve carbohydrate metabolism in *Saccharomyces cerevisiae*. *J Bacteriol* 1997;**179**:6560–5.

Stephanopoulos GN, Aristidou AA, Nielsen J. *Metabolic Engineering: Principles and Methodologies*. San Diego: Academic Press, 1998.

Theobald U. *Untersuchungen zur Dynamik des Crabtree-Effektes. Ph.D. Thesis*. Institut für Bioverfahrentechnik der Universität Stuttgart 1995.

Vanoni M, Vai M, Frascotti G. Effects of temperature on the yeast cell cycle analyzed by flow cytometry. *Cytometry* 1984;**5**:530–3.

Verduyn C, Postma E, Scheffers WA *et al.* Energetics of *Saccharomyces cerevisiae* in anaerobic Glucose-Limited chemostat cultures. *J Gen Microbiol* 1990;**136**:405–12.

Villadsen J, Nielsen J, Liden G. *Bioreaction Engineering Principles*. 3rd. ed. Springer, 2011, 1–561.

Zakhartsev M, Yang X, Pörtner HO *et al.* Metabolic efficiency in yeast *Saccharomyces cerevisiae* in relation to temperature dependent growth and biomass yield. *J Therm Biol* 2015;**52**:117–29.